ADVANCES IN ATMOSPHERIC SCIENCES, VOL. 25, NO. 3, 2008, 458–466

Spatio-temporal Variability of Northern Hemipheric Sea Level Pressure (SLP) and Precipitation over the Mid-to-Low Reaches of the Yangtze River

HAN Xue[1,3] (韩 雪), WEI Fengying*[2] (魏凤英), Yves M. TOURRE[4,5], and DONG Wenjie[3] (董文杰)

[1]*Institute of Atmospheric Physics, Chinese Academy of Sciences, Beijing* 100029

[2]*State Key Laboratory of Severe Weather, Chinese Academy of Meteorological Sciences, Beijing* 100081

[3]*State Key Laboratory for Earth Surface Processes and Resource Ecology, Beijing Normal University,* 100875

[4]*MEDIAS-France, Toulouse, France*

[5]*LDEO of Columbia University, New York, USA*

(Received 21 June 2007; revised 4 September 2007)

ABSTRACT

The spatio-temporal variability of Northern Hemisphere Sea Level Pressure (SLP) and precipitation over the mid-to-low reaches of the Yangtze River (PMLY) is analyzed jointly using the multi-taper /singular value decomposition method (MTM-SVD). Statistically significant narrow frequency bands are obtained from the local fractional variance (LFV) spectrum. Significant interdecadal (i.e., 16-to-18-year periods) and interannual (i.e., 3-to-6-year periods) signals are identified. Moreover, a significant quasi-biennial signal is identified but only for PMLY data. The spatial joint evolution of patterns obtained for peaks in the LFV spectrum sheds light on relationships between SLP and PMLY: the Arctic Oscillation (AO) modulates the variability of the PMLY while the interannual variability of PMLY is in phase with the Northern Atlantic Oscillation (NAO) and the Northern Pacific Oscillation (NPO).

Key words: MTM-SVD, coupled spatio-temporal characteristics

DOI: 10.1007/s00376-008-0458-x

1. Introduction

Numerous studies have identified the importance of anomalous precipitation over the mid-to-low reaches of the Yangtze River (PMLY). Anomalous PMLY is closely related to climate anomalies over the Yangtze-Huaihe region in China. The interdecadal variability of PMLY may be attributed to the climate external forcings (Trenberth and Hurrell, 1994; Li, 1998; Kawamura et al., 1995), and be associated with atmospheric interdecadal oscillations (Schlesinger and Ramankuty, 1994). Many factors contribute to the PMLY variability since global atmosphere-ocean interactions occur on multi-timescale variability (Tourre and White, 2006). In order to provide insights on possible mechanisms, relationships between anomalous PMLY and global climate variability, especially the ENSO and the Pacific Decadal Oscillation (PDO) in the northern Pacific, have been investigated (Xu and He, 2001; Xian and Li, 2003; Wei and Song, 2005). Results show that significant interannual and interdecadal ocean signals are associated with anomalous PMLY and climate signals which are associated with the Sea Level Pressure (SLP) cycles are the most direct and important factors causing anomalous PMLY. For example, the position, intensity and patterns of the west Pacific subtropical high pressure have a close relationship with anomalous PMLY (Gong et al., 2000). In recent years, more attention has been paid to the Antarctic Oscillation (AAO) and Arctic Oscillation (AO), which are both linked to the major annular modes in Southern Hemisphere and Northern Hemisphere. Earlier results indicate that there is a significant positive correlation between the winter AAO and PMLY in summer-

*Corresponding author: WEI Fengying, weify@cams.cma.gov.cn

time (Nan and Li, 2003; Yu and Chen, 2005; Gao et al., 2005); there is also a significant negative correlation between the winter AO and time lagged PMLY (Gong et al., 2000); finally the interdecadal variability of the PMLY is consistent with that of AO (Wei et al., 2006). However, correlations between key atmospheric parameters and PMLY datasets have been obtained using methods such as canonical correlation analysis (CCA) and singular value decomposition (SVD). The main weakness of these diagnostic methods is that they emphasize relationships between standing modes, but they can not be used to shed light on the dynamics of evolving signals.

The purpose of this paper is to investigate coupled spatio-temporal evolution of the PMLY and the Northern Hemispheric SLP using the multi-taper-method/singular value decomposition (MTM-SVD) technique which can reveal coherent spatial evolution of joint parameters. The MTM-SVD approach is based upon multivariate frequency-domain decomposition developed by Mann and Park (Mann and Park, 1999). The MTM-SVD can be used not only to detect dominant frequencies, but also to investigate possible dynamic correlation between two fields by reconstructing spatiotemporal patterns at given frequencies. The MTM-SVD method has been successfully used for signal detection and reconstruction of global temperature data over the past century, and decadal-to-century scale climate variability (Mann and Park, 1994; Mann et al., 1995). It has also been successfully applied in the investigation of joint spatio-temporal evolution of patterns involving two or more climate parameters (Mann and Park, 1996; Ribera and Mann, 2003; Zhang and Mann, 2005). Analyses of relationships between SLP and PMLY anomalous patterns using the above technique may provide physical insight into the underlying dynamical and physical mechanisms at interannual and interdecadal timescales.

2. Data and methods

2.1 *Data*

Monthly precipitation datasets for the period from January 1951 to December 2000 at 52 stations covering the mid-to-low reaches of the Yangtze River are used (Fig. 1). These datasets are taken from the National Meteorological Information Center and they passed quality control by the homogenization method. A Cressman objective analysis is performed on the station data to arrive at a gridded result that represents the station data. National Centers for Environmental Prediction (NCEP) reanalysis of SLP on a 5°×5° gridpoint system over the entire Northern Hemisphere are downloaded from the website (http://www.cdc.noaa.gov/cgi-bin/db_search/DBSea-rch.pl?Dataset=Search.pl?Dataset = CDC+Derived+NCEP+Reanalysis+Products + Surface + Level&Variable = Sea+level + pressure & Statistic = Mean &group=0&submit=Search), and for the same 50-year period are also analyzed.

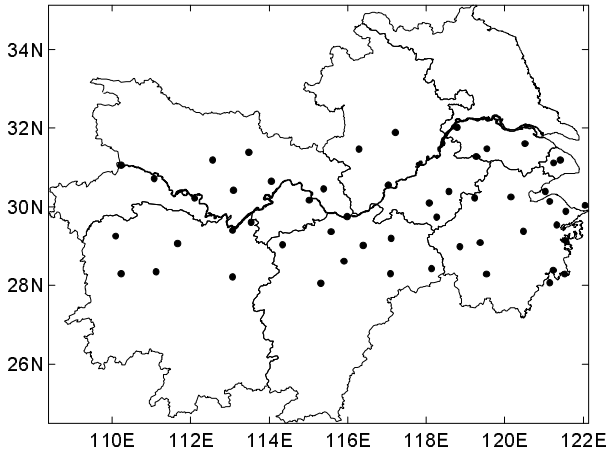

Fig. 1. The 52 rainfall stations over the mid-to-low reaches of the Yangtze River (PMLY).

2.2 *Methods*

The MTM-SVD method is described with details elsewhere (see for example Mann and Park, 1994, 1996, 1999). Basically to identify coherent structure across multivariate datasets, time-series are standardized first. The time-series are then transformed into the spectral domain (Thomson, 1982). The eigenspectra are thus:

$$Y_h(f) = \sum_{t=1}^{N} a_h(t) F(t) e^{2\pi i f t \Delta t}\,, \quad h = 1, \cdots, H\,. \quad (1)$$

Then values of H eigenspectra $\boldsymbol{Y}_{m,h}(f)$ are reorganized, $m = 1, \cdots, M$, for the M time-series and for each frequency f into a matrix $\boldsymbol{Y}(f)$ of dimension $M \times H$, through Fourier transform. A complex SVD is performed on the above matrix $\boldsymbol{Y}(f_0)$ and matrix $\boldsymbol{Y}(f_0)$ may be reconstructed as:

$$Y_{m,h}(f_0) = \sum_{k=1}^{K} U_{m,k}(f_0)\gamma_k(f_0)V_{k,h}(f_0)\,. \quad (2)$$

The K singular values $\gamma_k(f)$ scale the amplitude of each mode in this local decomposition. The first mode Local Fractional Variance (LFV) is defined as:

$$\mathrm{LFV} = \frac{\gamma_1^2(f)}{\sum_{k=1}^{K} \gamma_k^2(f)}\,. \quad (3)$$

Thus, within the LFV spectrum prominent peaks indicates the presence of a statistically significant signals. This provides a powerful tool for signals' detection in

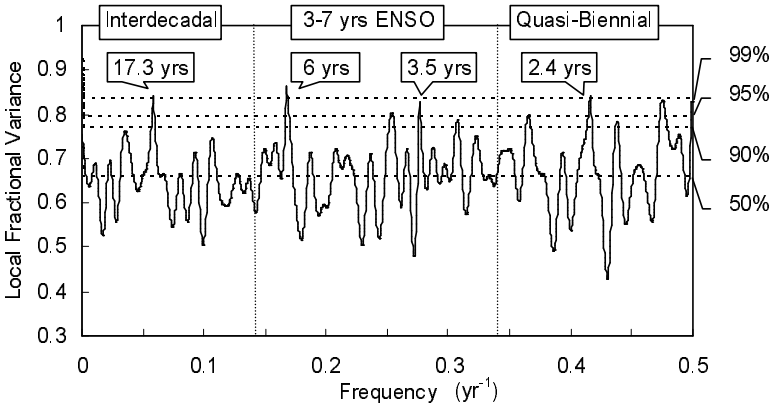

Fig. 2. The LFV spectrum of the PMLY. Horizontal dashed lines represent the 99%, 95%, 90% confidence levels. Vertical dashed lines represent the frequency-bands for the interdecadal, ENSO, and quasi-biennial signals, respectively.

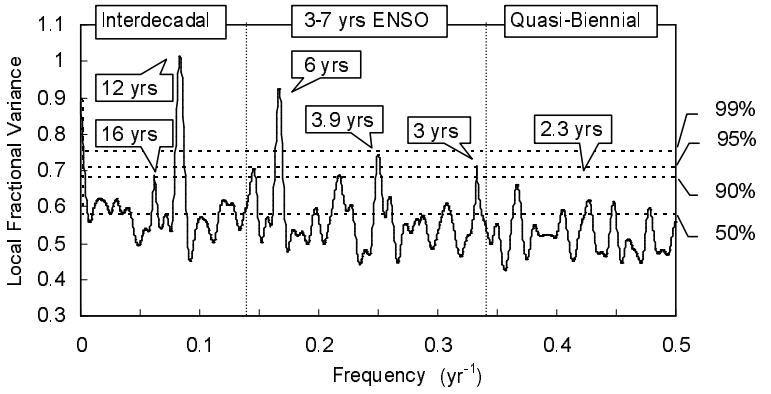

Fig. 3. The LFV spectrum of the Northern Hemisphere SLP. Dashed lines represent the 99%, 95%, 90% confidence levels. Vertical dashed lines represent the frequency bands for the interdecadal, ENSO, and quasi-biennial signals.

the frequency domain. We thus use LFV spectrum for the first modes with appropriate significance levels for signal detection. Significant confidence levels are estimated through a boot-strapping procedure (following Efron, 1990). Then the spatial and temporal patterns of the signal associated with the lead signals for a frequency are reconstructed, following:

$$F_{m,1}(t) = \delta(f_0)\Re\{\sigma_m U_{m,1}(f_0)\alpha_1(t)e^{-2\pi i f_0 t}\}\,. \quad (4)$$

The complex vector $U_{m,1}(f_0)$ of length M is the spatial first mode of the decomposition at f_0. It represents the spatial pattern of the signal at frequency f_0 and contains information about the relative phase and amplitude of the signal at all locations i of the multivariate datasets. $A_1(t) = \Re\{\alpha(t)e^{-2\pi i f_0 t}\}$ represents the temporal pattern of the signal at frequency f_0. It can be seen as a signal having a dominant oscillation at frequency f_0, where the variable amplitude $\alpha(t)$ represents the slowly varying envelope of the oscillatory signal.

3. The LFV spectral characteristics of the PMLY and the Northern Hemisphere SLP

The MTM-SVD approach (with three tapers) is applied separately on the PMLY and the SLP datasets to identify the timescales of statistically significant oscillatory signals from the LFVs spectra. LFV values were smoothed using the roughness boundary constraint method (see Mann, 2004).

The LFV spectrum of the PMLY is displayed in Fig. 2, with many robust peaks which indicate the multi-timescales variability of the PMLY. The peak near 17.3-year within the interdecadal frequency band (16.4–18-year period) reaches the 99% confidence level. This result is consistent with the previous study (Wei

Table 1. Key information from LFV individual spectra of the PMLY and the Northern Hemisphere SLP.

		Frequency (yr^{-1})	Periods (yr)	LFV	Confidence Level
PMLY	Trend	0	–	0.761	50%
	Interdecadal	5.86	17.06	0.8426	99%
	9–12 Year	10.57	9.46	0.7845	90%
	ENSO	16.80	6.0	0.8608	99%
	ENSO	30.69	3.25	0.8239	95%
	Quasi-Biennial	41.67	2.4	0.8463	99%
SLP	Trend	0	–	0.9309	99%
	Interdecadal	6.15	16.26	0.7055	90%
	9–12 Year	8.13	12.3	0.9832	99%
	ENSO	16.80	6.0	0.9225	99%
	ENSO	33.35	3.0	0.7138	95%
	Quasi-Biennial	42.85	2.3	0.6456	50%

and Zhang, 2004), indicating a statistically significant interdecadal band (16–18-year periods). The ENSO band (3–7-year periods) has two peaks at the 99% confidence level near 6-year and 3.5-year. Numerous investigations have identified that the 3.5- and 6-year oscillations, are associated with the interannual variability of the global climate system, particularly the ENSO signal (Allan et al., 1996; Reason and Mulenga, 1999; Tourre and White, 2006). The quasi-biennial (QB) band contributes significantly to the LFV spectrum, with a peak near 2.4-year reaching the 99% confidence level. The statistically significant quasi-biennial signal for the PMLY could be associated with that of the QBO (Kuaff, 1992) and could contribute to the quasi-biennial oscillatory mode of precipitation over China (Yang, 2006).

Maximum entropy spectrum (MES) and wavelet methods are also used for the analysis of the average precipitation time-series at the 52 stations (not shown). Analysis shows that only the 3-year period can be detected in the MES. The 17–18-year and 3–6-year band-periods appear in the wavelet analysis. In order to prove the reliability of the interdecadal oscillation of the PMLY for the 16–18-year periods, a power spectrum method is applied to the 101-year (1905–2005) precipitation datasets at Shanghai, Nanjing, Chengsi, Hangzhou, Wuhu, Wenzhou, Wuhan, Jiujiang, Jinzhou and Yichang stations over the mid-to-low reaches of the Yangtze River (not shown). Analysis indicates that the interdecadal signal is indeed statistically significant as in the MTM-SVD analyses of the PMLY datasets.

In Fig. 3 the individual LFV spectrum of Northern Hemisphere SLP is displayed. The interdecadal band has a peak near 16-year, significant at the 90% confidence level, and the peak near 12-year is significant at the 99% confidence level. Within the ENSO band, the peaks near 6-year, 3.9-year periods are significant at the 99% confidence level, and the peak near the 3-year period is significant at the 95% confidence level. However, the peaks near 2.3-year period within the QB band are significant at only the 50% confidence level.

The summary of the above two LFV spectra is listed in Table 1. Noted the QB signal for SLP is much weaker than that of PMLY. This may suggest that the QB signal for PMLY is related to other quasi-biennial oscillations from the atmosphere or the quasi-biennial oscillation in the atmosphere-ocean system over the Asia-Anzac monsoon (Mooley and Parthasarathy, 1984).

4. Coupled characteristics of the PMLY and the Northern Hemisphere SLP

As in previous joint MTM-SVD analyses (Mann and Park, 1996; Delworth and Mann, 2000; Ribera and Mann, 2002), the standardized grid point data were also weighted so that different fields contribute equally to the overall variance. Then the MTM-SVD method can identify coupled and coherent spatially-evolving signals, by using both phase and amplitude information.

4.1 *The interdecadal coupled characteristics of the PMLY and the Northern Hemisphere SLP*

Evolving spatio-temporal patterns of the joint PMLY-SLP associated with the statistically significant interdecadal timescale centered near the 18-year period identified in LFV spectrum are analyzed first.

The first mode accounts for ∼42% of the variance from the joint PMLY-SLP dataset. Figure 4 shows the evolution of the signal over one-half cycle (with increment of 2.2 year between snap shots). The joint mode analysis exhibits distinct spatial evolution at phase 0°, 45°, 90°, 135°, 180°. Beginning at phase 0° (Fig. 4a1), positive SLP anomalies are seen over high latitudes of Asia-Europe, North America and North

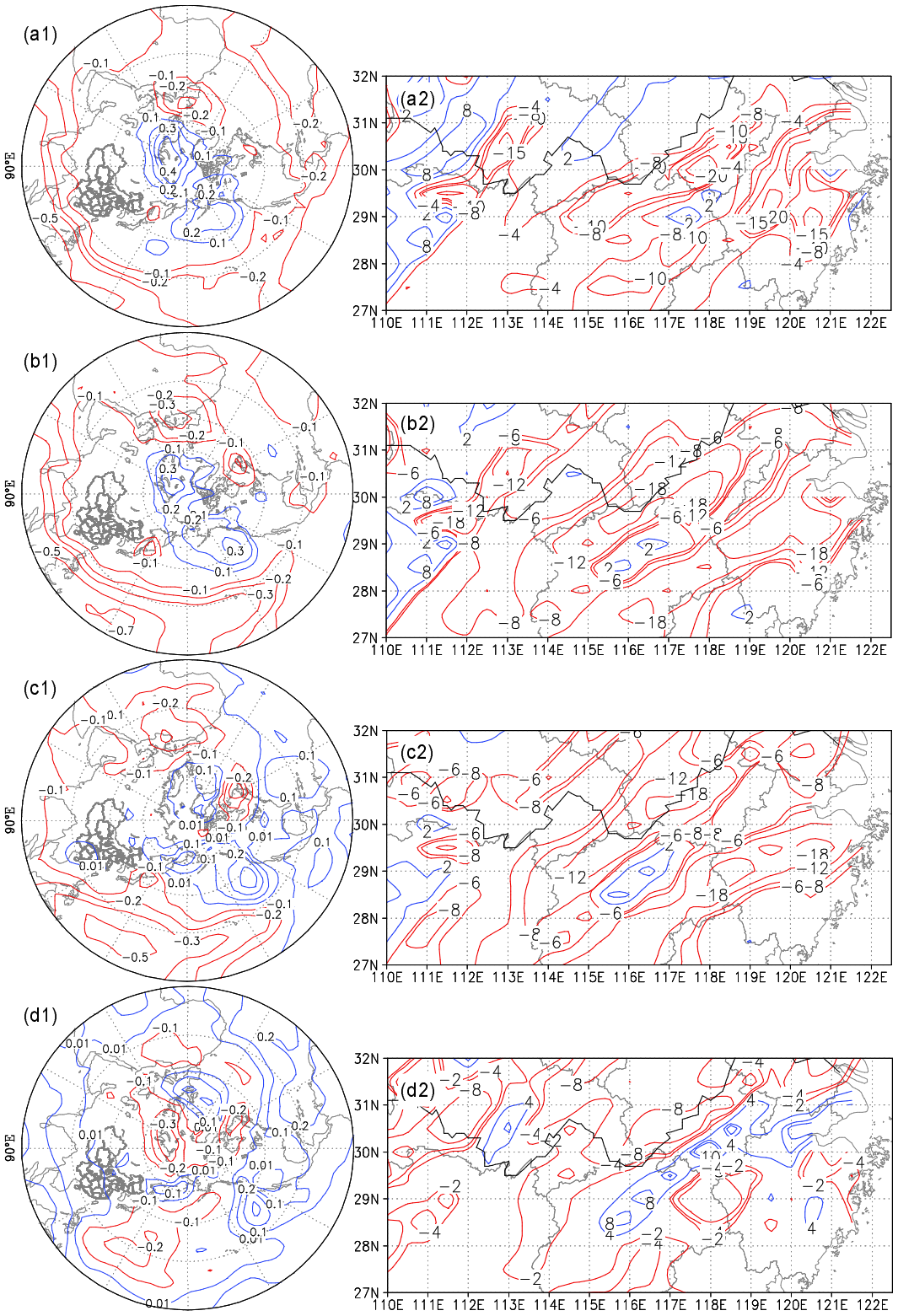

Fig. 4. Spatial reconstruction of joint PMLY-SLP evolution at interdecadal timescales. The left column is for SLP evolution (from a1 to d1) and the right column is for PMLY evolution (from a2 to d2), corresponding to spatial patterns at phases: 0°, 45°, 90°, and 135°, respectively (blue lines are for positive anomalies of both fields while red lines are for negative anomalies of both fields).

Pacific, while negative SLP anomalies are found at middle latitudes. The SLP patterns at phase 0° are similar to those of the negative AO phase. At phase 45° (Fig. 4b1), the areas with positive SLP anomalies are reduced in high latitudes, while negative SLP anomalies expand towards high latitudes. At phase 135° (Fig. 4d1), negative SLP anomalies are found at high latitudes, while positive SLP anomalies have developed in mid-latitudes. At phase 180° (9 year later) (not shown), the region of negative SLP anomalies encompasses the entire high latitudes; with the positive SLP anomalies are found only at mid-latitudes. The most prominent feature in the associated PMLY pattern is a large region of negative PMLY anomalies over the mid-lower reaches of the Yangtze River at phase 0° (Fig. 4a2), indicative of a drought signal. The overall phase changes of the PMLY are in phase with the AO. Through the evolution of the half cycle (not shown), positive precipitation anomalies dominate most parts of the mid-to-low reaches of the Yangtze River. The interdecadal (ID) SLP annular patterns or AO, seem to play a very important role on the interdecadal (ID) PMLY variability.

The temporal patterns of joint PMLY-SLP at ID timescale centered near the 18-year period are reconstructed for a grid point at 65°N, 30°E and compared to the Wuhan precipitation record. They are displayed in Figs. 5a and 5b. It can be seen that there is an obvious distinction between their interdecadal variability. The phase of PMLY lags that of SLP approximately 3–4 years. We calculate the lag cross correlation of PMLY and SLP. The reconstructed interdecadal SLP

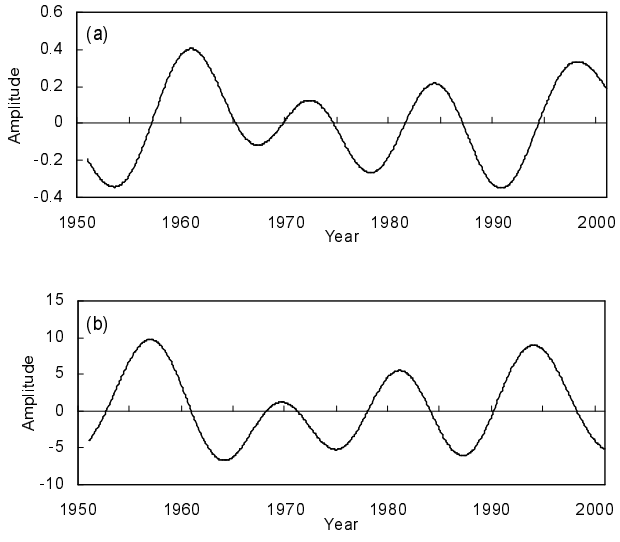

Fig. 5. Temporal reconstruction of the joint PMLY-SLP at interdecadal timescale. (a) temporal pattern of reconstructed SLP at the grid point 30°E, 65°N; (b) temporal pattern of reconstructed PMLY from Wuhan station.

weights at high latitudes are negatively correlated with PMLY at zero lag, with a very weak correlation coefficient of −0.14. Since the number of samples is 600, the correlation coefficient reaches the 0.001 confidence level. Results indicate that when low SLP is found at high latitudes, there is a tendency for the PMLY to enter into a rainy period, and vice versa. Nevertheless negative correlation lagged at 2, 3, 4, and 5 years are much more significant, with correlations of: −0.8, −0.9, −0.8, and −0.6, respectively. This shows that there might be a relationship with the strong 2-to-3 year and 4-year oscillations of the annular pressure anomalies at high latitudes (Yu and Chen, 2005).

4.2 *The interannual coupled characteristics of the PMLY and the Northern Hemisphere SLP*

The spatial patterns of the joint fields associate with the 3 year period in the LFV spectrum are reconstructed for a half-cycle with increment of 4 months between snap shots.

The first interannual mode accounts for 61% of the whole variance. The spatial evolutions are displayed in the Fig. 6, with the left column for SLP, and right column for PMLY, respectively. Starting at phase 0° (Fig. 6a1), the mode is associated with positive SLP anomalies in the Greenland, Iceland and the high latitudes from Siberian to North Canada, and the whole Arctic pole exhibits positive SLP anomalies, centered around the Greenland Sea. The negative SLP anomalies are found in middle and low latitudes, centered in the North Atlantic, subtropical and tropical Pacific. The SLP exhibits opposite phases between high and middle-low latitudes in the Northern Hemisphere. From phase 45° to phase 90° (Figs. 6b1 to 6c1), the observed SLP pattern weakens. The positive SLP anomalies decrease at the Arctic, and then high latitudes of North Atlantic and North Pacific become centers of negative SLP anomalies. At phase 135° (Fig. 6d1) the negative SLP anomalies expand towards the high latitudes over the entire Arctic, while positive SLP anomalies are in most part of middle-to-low latitudes. At phase 180° (not shown), negative SLP anomalies are found at high latitudes and positive SLP anomalies at middle-to-low latitudes (i.e., opposite phase pattern than at phase 0°). Negative SLP anomalies appeared over Iceland, Greenland, and high latitudes from East Siberia to northern Canada and positive SLP anomalies in the North Atlantic, subtropical, and tropical Pacific. This implies low layer atmospheric SLP reflecting that of both the North Atlantic Oscillation (NAO) and North Pacific Oscillation (NPO). In right column of Fig. 6 shows that negative PMLY anomalies are found almost everywhere at

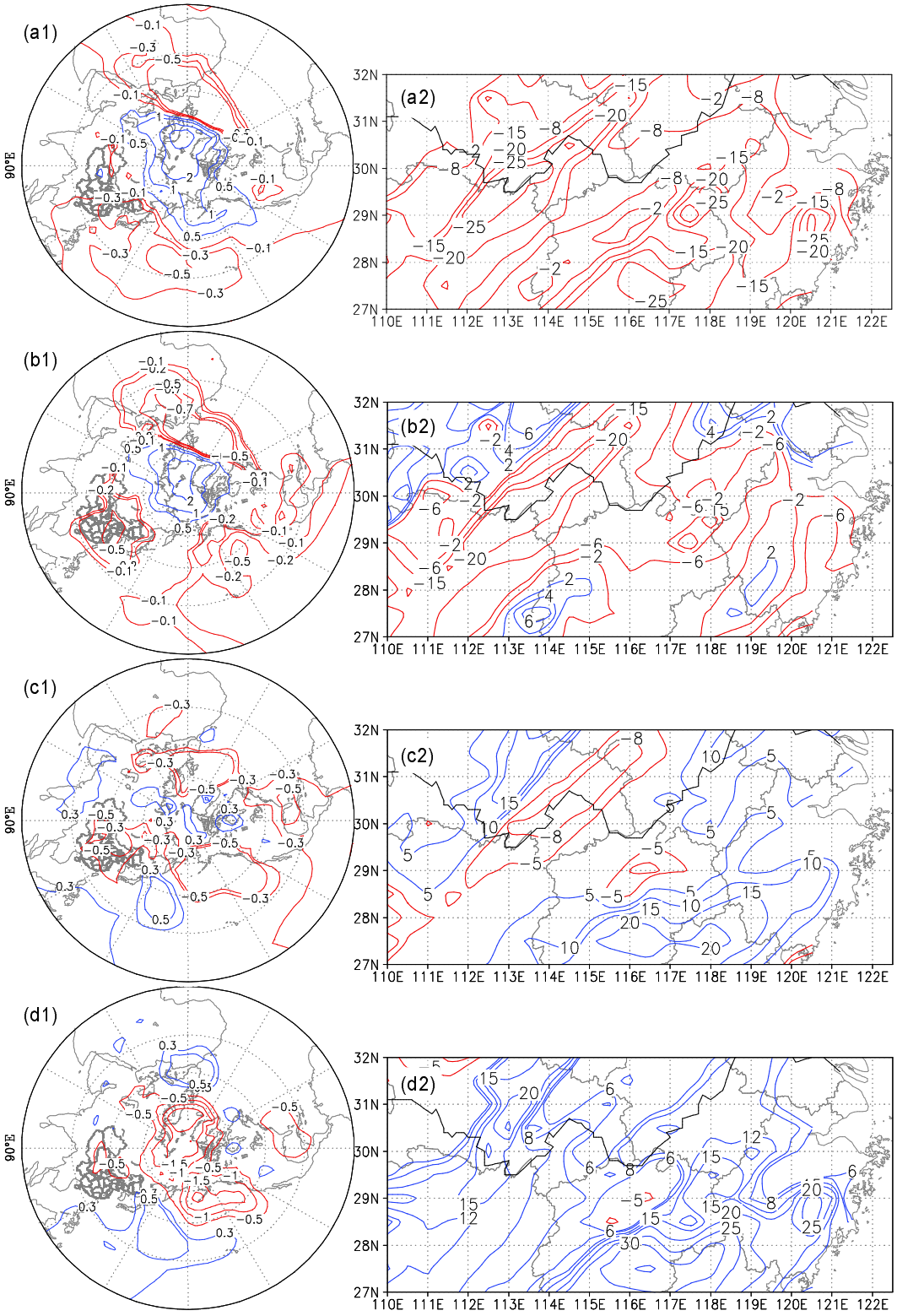

Fig. 6. Spatial reconstruction of joint PMLY-SLP evolution at interannual timescales. The left column is for SLP evolution (from a1 to d1) and the right column is for PMLY evolution (from a2 to d2), corresponding to spatial patterns at phases: 0°, 45°, 90°, and 135°, respectively (blue lines are for positive anomalies of both fields while red lines are for negative anomalies of both fields).

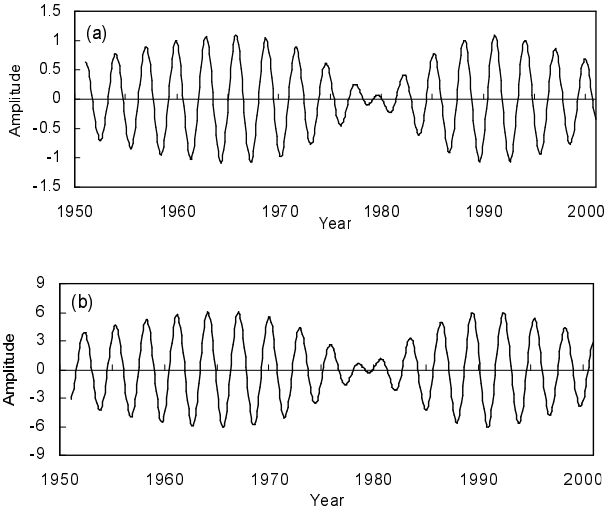

Fig. 7. Temporal reconstruction of the joint PMLY-SLP in interannual timescale. (a) temporal pattern of reconstructed SLP at the grid point 65°N, 30°E; (b) temporal pattern of reconstructed PMLY from Wuhan station.

phase 0° (Fig. 6a2) while decreasing at phase 45° onward (Fig. 6b2). From phase 90° onward (Fig. 6c2), positive anomalies are found in the northern and southern areas of the mid-to-low reaches of the Yangtze River. Rainy anomalies over the PMLY are thus associated with positive phases of both AO and NPO.

The reconstructions of temporal patterns at interannual timescales centered near the 3-year period are shown in Figs. 7a and 7b. Comparing the two time-series, it can be seen that there is a significant negative correlation of −0.92 between the interannual variability of SLP in high latitudes of Northern Hemisphere and the PMLY. It means that negative SLP anomaly in high latitudes are associated with positive PMLY anomaly, and vice-versa.

5. Conclusions

Analyses of Northern Hemisphere SLP and precipitation over mid-to-low reaches of Yangtze River, based on the MTM-SVD method, yield evidence of coherent oscillatory patterns of variability in the two fields. Both fields have statistically significant oscillatory signals at both interdecadal timescale from 16-to-18-year period and interannual timescale from 3-to-6 year period. In addition, a significant QB signal is found for PMLY only. However, the secular trend of SLP is more significant than that of the PMLY. This indicates that the anomalous variability of the PMLY may be associated with other atmosphere-ocean coupled signals.

The coupled spatiotemporal patterns of the above signals show a close relationship between SLP and PMLY. For the interdecadal timescale, the PMLY anomalies evolve from a drought to a rainy period is in phase with that of the AO from negative phase to positive phase, corresponding results from (Wei et al., 2006). For interannual timescale, the NAO and NPO anomalies are found of being linked with PMLY anomalies.

Acknowledgements. This research is supported by The National Natural Science Found of China under Grant No. 40575057 and No. 40275020. The authors would like to thank Dr. Michael E. Mann [Associate Professor and Director of Earth System Science Center (ESSC), PennState University], and Yves M. Tourre would like also to thank Dr. Mike Purdy (Director of LDEO of Columbia University), Dr. Arnold Gordon (Department of Physical Oceanography at LDEO), Dr. Jean-Claude André (Director of CERFACS), and Dr. Patrick Van-Grunderbeeck (Director of MEDIAS-France), for their continuing support. This is LDEO contribution No. 7138.

REFERENCES

Allan, R., J. Lindesay, and D. Parker, 1996: *El Niño-Southern Oscillation and Climate Variability*. CSIRO Publishing, Collingwood, AU, 405pp.

Delworth, T. L., and M. E. Mann, 2000: Observed and simulated multidecadal variability in the Nothern Hemisphere. *Climate. Dyn.*, **16**, 661–676.

Efron, B., 1990: *The Jackknife, the Bootstrap and Other Resampling Plans*. Society for Applied and Industrial Mathematics, Philadelphia, 92pp.

Gao, H., F. Xue, and H. J. Wang, 2005: The effect of the interannual variation of the Antarctic oscillation on the rainfall along Changjiang-Huaihe River and its forecasting significance. *Chinese Science Bulletin*, **48**(suppl.), 87–92.

Gong, D. Y., J. H. Zhu, and S. W. Wang, 2000: Significant relationship between spring AO and the summer rainfall along the Yangtze River. *Chinese Science Bulletin*, **47**(7), 546–549.

Kawamura, R., M. Sugi, and N. Sato, 1995: Interdecadal and interannual variability in the northern extratropical circulation simulated with the JMA global model. Part I: Wintertime leading mode. *J. Climate*, **8**, 3006–3019.

Kuaff, J. A., 1992: The Modulation of Monsoon Intensity by Stratospheric QBO. *Proc. Seventeenth Annual Interannual Climate Diagnostic Workshop*, Norman, OK, 19–23 October, 306–311.

Li, C. Y., 1998: The quasi-decadal oscillation of air-sea system in the northwestern Pacific region. *Adv. Atmos. Sci.*, **15**, 31–40.

Mann, M. E., 2004: On smoothing potentially non-stationary climate time series. *Geophys. Res. Lett.*, **31**, L07214, doi: 10.1029/2004GL019569.

Mann, M. E., and J. Park, 1994: Global-scale modes of surface temperature variability on interannual to interannual to century timescales. *J. Geophys. Res.*, **99**(D12), 25819–25833.

Mann, M. E., and J. Park, 1996: Joint Spatio-Temporal modes of surface temperature and sea level pressure variability in the Northern Hemisphere during the last century. *J. Climate*, **9**, 2137–2162.

Mann, M. E., and J. Park, 1999: Oscillatory spatiotemporal signal detection in climate studies: A multiple-taperspectral domain approach. *Advances in Geophys*, **41**, 1–131.

Mann, M. E., U. Lall, and B. Saltzman, 1995: Decadal-to-century scale climate variability: Insights into the Rise and Fall of the Great Salt Lake. *Geophys. Res. Lett.*, **22**, 937–940.

Mooley, D. A., and B. Parthasarathy, 1984: Fluctuations in all-India summer monsoon rainfall during 1871–1978. *Climatic Change*, **6**, 287–301.

Nan, S. L., and J. P. Li, 2003: The relationship between the summer precipitation in the Yangtze River valley and the boreal spring Southern Hemisphere interannual mode. *Geophys. Res. Lett.*, **30**(20), 2266.

Reason, C. J. C., and H. M. Mulenga, 1999: Relationships between South African rainfall and SST anomalies in the South West Indian Ocean. *International Journal of Climatology*, **19**, 1651–1673.

Ribera, P., and M. E. Mann, 2002: Interannual variability in the NCEP Reanalysis 1948–1999. *Geophys. Res. Lett.*, **29**(10), 1494, doi:10.1029/2001GL013905.

Ribera, P., and M. E. Mann, 2003: ENSO related variability in the Southern Hemisphere 1948–2000. *Geophys. Res. Lett.*, **30**(1), 1006, doi: 10.1029/2002GL015818.

Schlesinger, M. E., and N. Ramankuty, 1994: An oscillation of global climate system of period 65–70 years. *Nature*, **367**, 723–726.

Thomson, D. J., 1982: Spectrum estimation and harmonic analysis. *IEEE Proc*, **70**, 1055–1160.

Tourre, Y. M., and W. B. White, 2006: Global climate signals and equatorial SST variability in the Indian, Pacific and Atlantic oceans during the 20th century. *Geophys. Res. Lett.*, **33**(6), L06716, doi: 10.1029/2005GL025176.

Trenberth, K. E., and J. W. Hurrell, 1994: Decadal atmosphere-ocean variations in the Pacific. *Climate Dyn.*, **9**, 303–319.

Wei, F. Y., and J. J. Zhang, 2004: Climatic variation of Meiyu in the middle-lower reaches of Changjing River during 1885–2000. *Journal of Applied Meteorological Science*, **15**(3), 313–321. (in Chinese)

Wei, F. Y., and Q. Y. Song, 2005: Spatial distribution of the Global sea surface temperature with interdecadal scale and their potential influence on Meiyu in middle and lower reaches of Yangtze River. *Acta Meteorologica Sinica*, **63**(4), 477–484. (in Chinese)

Wei, F. Y., Q. Y. Song, and X. Han, 2006: Influence of spatial distribution of the sea level pressure in Northern Hemispere in the last 100 years on Meiyu over middle and lower reachers of Changjiang River. *Progress in Natural Science*, **16**(2), 215–222. (in Chinese)

Xu, H. M., and J. H. He, 2001: Interannual variability of the Meiyu onset and its association with North Atlantic oscillation and SSTA over North Atlatic. *Acta Meteorologica Sinica*, **59**(6), 694–706. (in Chinese)

Xian, P., and C. Y. Li, 2003: Interdecadal modes of sea surface temperature in the North Pacific Ocean and its evolution. *Chinese J. Atmos. Sci.*, **27**(5), 861–868. (in Chinese)

Yang, Q. M., 2006: Interdecadal variations of connections between the principal biennial oscillation pattern of rain in China and Global 500hPa circulation. *Chinese J. Atmos. Sci.*, **30**(1), 131–145. (in Chinese)

Yu, Y. Q., and W. Chen, 2005: *Influence of Air-sea Interaction on Climatic Change in China*. China Meteorological Press, Beijing, 177–197. (in Chinese)

Zhang, Z. H., and M. E. Mann, 2005: Coupled patterns of spatiotemporal variability in Northern Hemisphere sea level pressure and conterminous U. S. drought. *J. Geophys. Res.*, **110**, D03108, doi: 10.1029/2004JD004896.